CrystEngComm

COMMUNICATION

View Article Online
View Journal | View Issue

Cite this: *CrystEngComm*, 2014, **16**, 4959

Received 28th March 2014,
Accepted 25th April 2014

DOI: 10.1039/c4ce00647j

www.rsc.org/crystengcomm

Dynamic 2D manganese(II) isonicotinate framework with reversible crystal-to-amorphous transformation and selective guest adsorption†

Dariusz Matoga,*[a] Barbara Gil,[a] Wojciech Nitek,[a] Alexander D. Todd[b] and Christopher W. Bielawski[bc]

A 2D layered microporous isonicotinate-supported manganese(II) metal–organic framework was found to exhibit a reversible crystal-to-amorphous transformation upon the removal and uptake of certain guest molecules. Unsaturated metal centers, generated in the dynamic framework upon activation, were found to facilitate the selective adsorption of CO_2 *versus* N_2.

The design and synthesis of porous coordination polymers (PCPs) or metal–organic frameworks (MOFs) has been a rapidly expanding area of materials chemistry and nanotechnology over the past decade.[1,2] The attraction to the aforementioned materials is primarily due to a high crystallinity combined with a well defined porosity that results in abilities to accommodate guest molecules and enables applications in storage, separations, sensing and catalysis.[1,2] MOFs are often classified according to how the framework responds upon the removal of guest molecules.[3] The most recently recognized group, which are often called third-generation compounds or soft porous crystals, respond in a dynamic manner.[3,4] Indeed, the combination of framework flexibility and structural regularity opens possibilities of realizing unique properties not observed in conventional MOFs.[4]

MOFs are of great interest as new materials for CO_2 capture, which is directly related to clean energy and environmental protection.[2] High CO_2 uptake capacity and high CO_2/N_2 selectivity are among the desirable features of these materials. At high pressures, MOFs with large surface areas are shown to enhance capacity; however, at low pressures, a significant density of high-affinity adsorption sites, such as unsaturated metal centers (UMCs), have been shown to be an important factor.[2] Indeed, in addition to linker modification (*e.g.*, through the incorporation of Lewis-base or other functional sites), the introduction of UMCs into MOFs is an important strategy to improve the selective adsorption of CO_2.[2]

Herein, we report a third-generation two-dimensional (2D) microporous $\{[Mn_2(ina)_4(H_2O)_2]\cdot 2EtOH\}_n$ (**1as**; ina = isonicotinate; EtOH = ethanol) MOF, which was prepared *in situ* by combining isoniazid with Mn^{II} salts (see ESI†).[5] In contrast, a conventional synthesis from isonicotinic acid afforded a structurally and compositionally different product (**2**) (see Fig. S1†). The formation of **2** is favoured under kinetic control whereas **1as** is the thermodynamic product, formation of which is facilitated by low concentration of isonicotinate ions and lower reaction temperatures. It is also noteworthy that the synthesis using isoniazid is scalable and may be performed under mild conditions unlike many solvothermal methods used for the preparation of other related but rare Mn^{II} compounds with isonicotinate anions and/or ethanol/water guests.[6] The resulting air-stable framework exhibits unsaturated metal sites upon activation and was found to selectively adsorb CO_2 *versus* N_2. Indeed, the features of **1as** address two main challenges that have curtailed many practical applications of MOFs: cost and stability in the presence of water vapor.[2]

Single-crystal XRD revealed that the isonicotinate ligands in **1as** function as μ_3 and μ_2 linkers between the carboxylate-bridged dinuclear Mn^{II} clusters and act as nodes in the layered framework of a (4,4)-topology (Fig. 1 and S2–S3†).‡ The framework also exhibits 1D channels of approximately 3.7 × 2.9 Å^2, which were occupied by EtOH guest molecules. The non-polar ethyl groups were directed inside the 10.8 Å-thick layers. In contrast, the hydroxyl groups of the ethanol units were involved in strong hydrogen-bonds (O–H···O distances ranging from 2.666 to 2.786 Å) with both the framework free carboxylate groups and the coordinated H_2O guest

[a] *Faculty of Chemistry, Jagiellonian University, Ingardena 3, 30-060 Kraków, Poland. E-mail: matoga@chemia.uj.edu.pl; Fax: +48 12 6340515; Tel: +48 12 6632223*
[b] *Department of Chemistry, The University of Texas at Austin, 1 University Station, A1590, Austin, TX 78712, USA*
[c] *Department of Chemistry, Ulsan National Institute of Science and Technology, 50 UNIST-gil, Ulju-gun, Ulsan, 689-798, South Korea*

† Electronic supplementary information (ESI) available: Experimental details, synthetic procedures, crystallographic tables, additional figures, additional *in situ* IR spectra, TGA/QMS data, H_2 adsorption isotherm, UV-vis diffuse reflectance spectra and additional PXRD patterns. CCDC 938235 (**1as**). For ESI and crystallographic data in CIF or other electronic format see DOI: 10.1039/c4ce00647j

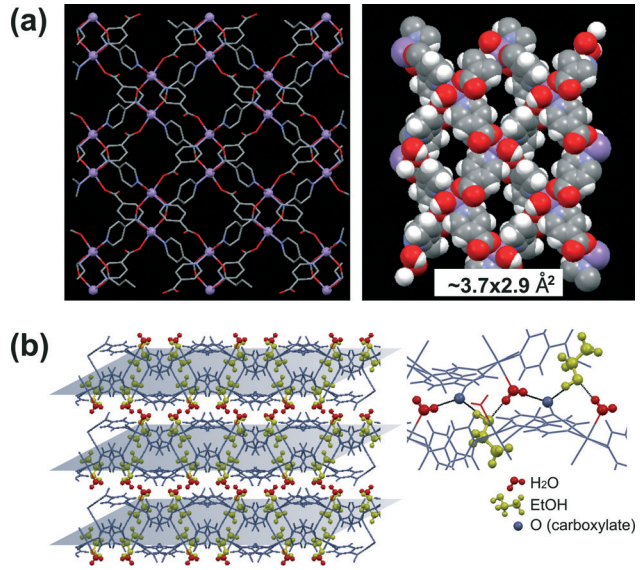

Fig. 1 Crystal structure of 2D $\{[Mn_2(ina)_4(H_2O)_2]\cdot 2EtOH\}_n$ MOF (**1as**). (a) Single layer with dinuclear Mn_2 nodes and their fourfold connectivity with isonicotinate linkers (EtOH guest molecules have been omitted for clarity) (left) viewed along the crystallographic *a* axis (H atoms omitted), and (right) represented in a spacefill model showing rectangular open channels. Mn, O, N, C, and H atoms are shown in purple, red, blue, gray and white, respectively. (b) Stacked layers viewed along the crystallographic *c* axis. (left) Coordinated H_2O molecules occupying the interlayer region and EtOH guest molecules are clearly visible. (right) Sequence of interlayer hydrogen-bonds involving H_2O, EtOH and framework free oxygen atoms of carboxylate groups, is indicated (black line).

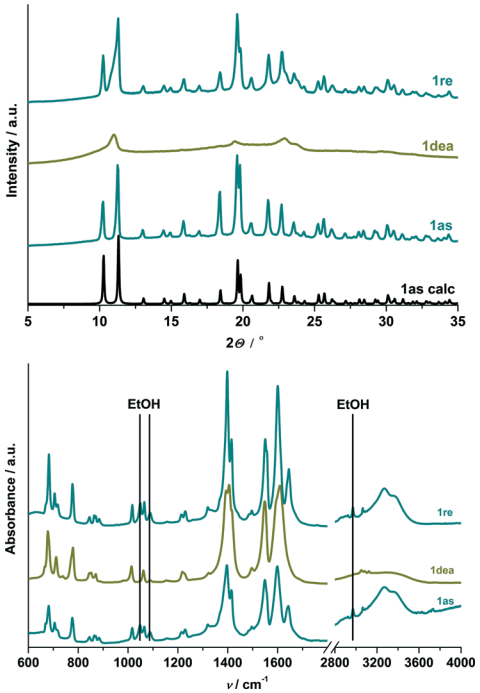

Fig. 2 PXRD patterns (top) and IR spectra (bottom) of the as-synthesized $\{[Mn_2(ina)_4(H_2O)_2]\cdot 2EtOH\}_n$ (**1as**), dried for 1 h at 150 °C followed by exposure to air at room temperature (**1dea**), and resoaked for 1 h at 50 °C in EtOH (**1re**). For comparison, PXRD pattern calculated from the single-crystal structure of **1as** is given (**1as calc**).

molecules. The structural flexibility of the framework arises from its interlayer hydrogen-bonding acceptor sites and labile guest molecules that can be readily and selectively removed (Scheme S1†). Moreover, the structure of **1as** is different from other reported compounds obtained from isonicotinic acid or aldehyde and various manganese(II) salts (*i.e.*, nitrates, perchlorates, chlorides).[6,7] Collectively, these observations underscore the importance of the synthetic conditions used to prepare isonicotinate-supported Mn^{II} materials.

The removal of EtOH guest molecules from **1as** was found to lead to the loss of long-range ordering in the material as the relative position of the adjacent layers were no longer stabilized through hydrogen-bonds and the layers were able to slide past each other. Such amorphous character of the framework (**1dea**) was revealed by PXRD analysis, as shown in Fig. 2. The reduced crystallinity of **1as** was fully recovered upon resoaking (**1dea**) in ethanol, which lead to **1re**, a material that was structurally and compositionally identical to **1as** (Fig. 2).

IR spectroscopy of the aforementioned materials revealed that the vibrations of the skeletal atoms remained intact during the aforementioned process, confirming the retention of the 2D framework structure (Fig. 2). In this cycle, disappearance and reappearance of bands attributed to EtOH molecules (and corresponding to C–O and aliphatic C–H stretching vibrations) were observed. Additionally, changes occurring within the ν(COO) region may be explained in terms of carboxylate involvement in the hydrogen-bonds with the EtOH guest molecules.

To the best of our knowledge, **1as** is the first reported homometallic manganese-based framework exhibiting a reversible crystal-to-amorphous transformation. Two mixed-metal manganese containing frameworks with such a transition have been reported,[8] and the known manganese-based frameworks with isonicotinate ligands have been observed to remain crystalline upon desolvation.[6a,b] The reversible **1as**–**1dea**–**1re** solid-state transition may be followed by either IR or UV-vis spectroscopy (Fig. 2 and S4–S5†) and offers the possibility of using **1as** as a sensor for ethanol detection.

Thermal activation of **1as** in air followed by the uptake of H_2O/EtOH from the liquid phase was successfully extended to an *in situ* IR spectroscopy study of the uptake of selected molecules from their gas phase. The sample of **1as** was stepwise desorbed at increasing temperatures under vacuum in the temperature region where the TGA data (Fig. S6†) indicated that only water and ethanol desorption occurred. Interestingly, under static conditions, water was removed more readily than ethanol, which was not reflected by the TGA measurement carried out under flow conditions (Fig. 3). Most likely, the kinetic diameter of water (2.7 Å), which is smaller than that of ethanol (4.5 Å) as well as smaller than a micropore window size, facilitated the diffusion of the former.[9] The decrease of water and alcohol IR bands may also be observed at lower wavenumbers. The band at 720 cm^{-1} attributed

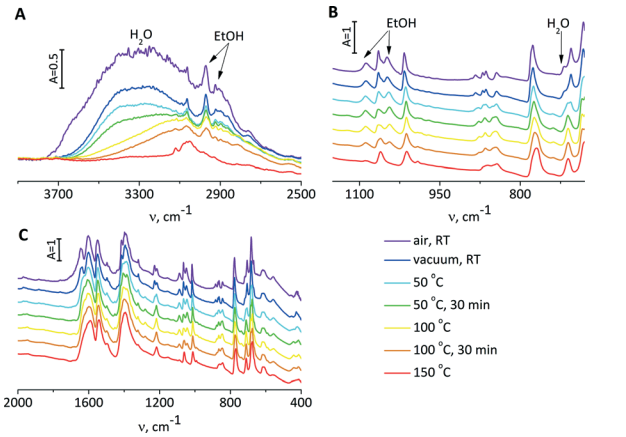

Fig. 3 *In situ* IR spectra recorded during activation of $\{[Mn_2(ina)_4(H_2O)_2]\cdot 2EtOH\}_n$ (**1as**) at increasing temperatures. A – region of OH and CH stretching vibrations, B – region of skeletal vibration showing stepwise desorption of water and ethanol, C – region of skeletal vibrations.

to water decreased at lower temperatures while two bands at 1047 and 1087 cm^{-1}, characteristic of alcohol C–O vibrations, exhibit diminished intensity at higher activation temperatures. The order–disorder phase change during solvent removal is not significantly reflected in IR spectroscopy, indicating that the short-order relations are not changed, *i.e.* the linker structure does not change upon spatial arrangement.

The activated sample of **1as** (after water and ethanol removal) has been studied as a potential adsorbent for carbon dioxide (Fig. 4). The *in situ* IR spectroscopy clearly shows that the MOF adsorbs CO_2 at −60 °C, near the CO_2 triple point. The sample also exhibited a new IR maximum at 2334 cm^{-1}, of lower wavenumber than free CO_2 (2345 cm^{-1}), indicating a slight weakening of C–O bonds, probably by direct interaction with open manganese sites (unsaturated metal centers). The interaction is relatively weak and, under ambient conditions, the sample does not retain the adsorbed CO_2. In addition, the presence of the adsorbed CO_2 does not change the activated MOF structure, which was confirmed by IR spectroscopy. Collectively, these results support the hypothesis that the CO_2 capture occurs when the exposed metal centers are generated in the sample and the presence

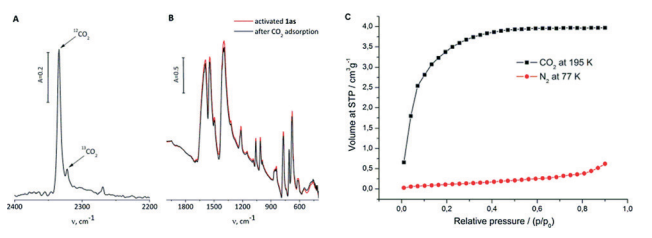

Fig. 4 Selective CO_2 *vs.* N_2 adsorption for activated $\{[Mn_2(ina)_4(H_2O)_2]\cdot 2EtOH\}_n$ (**1as**). (left) *In situ* IR spectra recorded during CO_2 adsorption at 213 K. A – region of C–O vibrations, B – region of skeletal vibrations. (right) CO_2 and N_2 adsorption isotherms at 195 K and 77 K, respectively.

of coordinated water molecules prevents this process. The important role of exposed manganese(II) centers in MOFs for selective sorption and catalytic processes has been previously emphasized in the literature.[10] Interestingly, while being active for CO_2 capture, the activated **1as** adsorbs N_2 only to a very limited extent, which was confirmed by isothermal adsorption measurements (Fig. 4). The CO_2/N_2 selectivity is a desirable feature of **1as** in the context of its potential use in flue gas separations (the selectivity factor of 9.3 was estimated at various temperatures and at partial pressures of 0.15 bar for CO_2 and 0.75 bar for H_2, see ESI†). More broadly, very few examples of such selectivity have been reported for metal–organic frameworks containing manganese(II) centers.[11]

In summary, the unique synthesis and the X-ray crystal structure of the layered isonicotinate-based manganese(II) metal–organic framework (**1as**) is reported. The framework was shown to expose metal centers upon reversible vacuum and/or thermal activation. The activation process was accompanied by a reversible crystal-to-amorphous transformation and enabled the MOF to selectively capture CO_2 *versus* N_2, and other gas separation applications. Additionally, the reversible solid-state transformation creates opportunities for using **1as** as a sensor for ethanol. Further post-synthetic modifications of this material are currently underway.

DM gratefully acknowledges National Science Centre in Poland (grant no. 2012/07/B/ST5/00904) for the financial support of this research. The research was carried out partially with the equipment purchased thanks to the financial support of the European Regional Development Fund in the framework of the Polish Innovation Economy Operational Program (contract no. POIG.02.01.00-12-023/08). CWB is grateful to the National Science Foundation (grant no. CHE-1266323) for support.

Notes and references

‡ $C_{14}H_{16}MnN_2O_6$, M = 363.23, monoclinic, a = 10.869(5), b = 12.130(5), c = 13.783(4) Å, β = 117.75(2)°, U = 1608.2(11) Å^3, T = 293(2) K, space group $P2_1/c$, Z = 4, 22 994 reflections measured, 3093 unique ($R_{(int)}$ = 0.0405). Final R indices [$I > 2\sigma(I)$] R = 0.0329, wR_2 = 0.0832.

1 For recent comprehensive reviews on MOFs and their applications, see thematic issues: (*a*) *Chem. Rev.*, 2012, **112**, 673–1268; (*b*) *Chem. Soc. Rev.*, 2011, **40**, 453–1152.

2 For recent comprehensive reviews on CO_2 capture based on MOFs, see: (*a*) Z. Zhang, Y. Zhao, Q. Gong, Z. Li and J. Li, *Chem. Commun.*, 2013, **49**, 653; (*b*) K. Sumida, D. L. Rogow, J. A. Mason, T. M. McDonald, E. D. Bloch, Z. R. Herm, T.-H. Bae and J. R. Long, *Chem. Rev.*, 2012, **112**, 724; (*c*) J. Liu, P. K. Thallapally, B. P. McGrail, D. R. Brown and J. Liu, *Chem. Soc. Rev.*, 2012, **41**, 2308; (*d*) J.-R. Li, Y. Ma, M. C. McCarthy, J. Sculley, J. Yu, H.-K. Jeong, P. B. Balbuena and H.-C. Zhou, *Coord. Chem. Rev.*, 2011, **255**, 1791.

3 (*a*) S. Kitagawa and K. Uemura, *Chem. Soc. Rev.*, 2005, **34**, 109; (*b*) K. Uemura, R. Matsuda and S. Kitagawa, *J. Solid*

State Chem., 2005, **178**, 2420; (*c*) S. Kitagawa and M. Kondo, *Bull. Chem. Soc. Jpn.*, 1998, **71**, 1739.

4 (*a*) G. Ferey and C. Serre, *Chem. Soc. Rev.*, 2009, **38**, 1380; (*b*) S. Horike, S. Shimomura and S. Kitagawa, *Nat. Chem.*, 2009, **1**, 695.

5 The conversion of isoniazid to isonicotinic acid in the presence of manganese centers may proceed *via* oxidation or hydrolysis pathways: (*a*) N. Nguyen, C. Claparols, J. Bernadou and B. Meunier, *C. R. Chim.*, 2002, **5**, 325; (*b*) J. Bodiguel, J. M. Nagy, K. A. Brown and B. Jamart-Gregoire, *J. Am. Chem. Soc.*, 2001, **123**, 3832.

6 (*a*) W. Lin, O. R. Evans and G. T. Yee, *J. Solid State Chem.*, 2000, **152**, 152; (*b*) R. Hauptmann, M. Kondo and S. Kitagawa, *Z. Kristallogr. - New Cryst. Struct.*, 2000, **215**, 171; (*c*) Q. Wei, M. Nieuwenhuyzen and S. L. James, *Microporous Mesoporous Mater.*, 2004, **73**, 97; (*d*) D. Huang, W. Wang, X. Zhang, C. Chen, F. Chen, Q. Liu, D. Liao, L. Li and L. Sun, *Eur. J. Inorg. Chem.*, 2004, 1454; (*e*) J.-H. Yu, J. Lu, Y. Xu, X. Zhang and J.-Q. Xu, *Inorg. Chim. Acta*, 2006, **359**, 3205.

7 For a deuterated analogue of **1as** obtained under solvothermal conditions, see: W. Dai, *Acta Crystallogr., Sect. E: Struct. Rep. Online*, 2008, **64**, m1032.

8 (*a*) J. Ferrando-Soria, R. Ruiz-Garcia, J. Cano, S.-E. Stiriba, J. Vallejo, I. Castro, M. Julve, F. Lloret, P. Amoros, J. Pasan, C. Ruiz-Perez, Y. Journaux and E. Pardo, *Chem. – Eur. J.*, 2012, **18**, 1608; (*b*) I. Imaz, G. Bravic and J.-P. Sutter, *Dalton Trans.*, 2005, 2681.

9 (*a*) H. Wu, Q. Gong, D. H. Olson and J. Li, *Chem. Rev.*, 2012, **112**, 836; (*b*) T. Borjigin, F. Sun, J. Zhang, K. Cai, H. Ren and G. Zhu, *Chem. Commun.*, 2012, **48**, 7613.

10 (*a*) M. Dincă, A. Dailly, Y. Liu, C. M. Brown, D. A. Neumann and J. R. Long, *J. Am. Chem. Soc.*, 2006, **128**, 16876; (*b*) M. Dincă, A. F. Yu and J. R. Long, *J. Am. Chem. Soc.*, 2006, **128**, 8904; (*c*) S. Horike, M. Dincă, K. Tamaki and J. R. Long, *J. Am. Chem. Soc.*, 2008, **130**, 5854; (*d*) L.-G. Qiu, L.-N. Gu, G. Hu and L.-D. Zhang, *J. Solid State Chem.*, 2009, **182**, 502; (*e*) T. K. Maji, S. Pal, K. L. Gurunatha, A. Govindaraj and C. N. R. Rao, *Dalton Trans.*, 2009, 4426; (*f*) Z.-B. Han, R.-Y. Lu, Y.-L. Zhou, Q. Chen and M.-H. Zeng, *Inorg. Chem.*, 2012, **51**, 674; (*g*) K. Sumida, D. Stück, L. Mino, J.-D. Chai, E. D. Bloch, O. Zavorotynska, L. J. Murray, M. Dincă, S. Chavan, S. Bordiga, M. Head-Gordon and J. R. Long, *J. Am. Chem. Soc.*, 2013, **135**, 1083.

11 (*a*) E. Jeong, W. R. Lee, D. W. Ryu, Y. Kim, W. J. Phang, E. K. Koh and C. S. Hong, *Chem. Commun.*, 2013, **49**, 2329; (*b*) P. Kar, R. Haldar, C. J. Gomez-Garcia and A. Ghosh, *Inorg. Chem.*, 2012, **51**, 4265; (*c*) D. N. Dybtsev, H. Chun, S. H. Yoon, D. Kim and K. Kim, *J. Am. Chem. Soc.*, 2004, **126**, 32.

